Proc. Natl. Acad. Sci. USA
Vol. 95, pp. 5372–5377, April 1998
Physiology

Targeted inactivation of *Npt2* in mice leads to severe renal phosphate wasting, hypercalciuria, and skeletal abnormalities

LAURENT BECK*, ANDREW C. KARAPLIS†, NORIO AMIZUKA‡, A. STACY HEWSON*, HIDEHIRO OZAWA‡, AND HARRIET S. TENENHOUSE*§

*Departments of Pediatrics and Human Genetics, McGill University, Montreal Children's Hospital Research Institute, Montreal, PQ, Canada H3H 1P3; †Division of Endocrinology, Sir Mortimer B. Davis-Jewish General Hospital, Lady Davis Institute for Medical Research, Department of Medicine, McGill University, Montreal, PQ Canada H3T 1E2; and ‡First Department of Oral Anatomy, Niigata University School of Dentistry, Niigata 951-8514, Japan

Edited by Darwin J. Prockop, MCP-Hahnemann Medical School, Philadelphia, PA, and approved February 18, 1998 (received for review November 18, 1997)

ABSTRACT ***Npt2* encodes a renal-specific, brush-border membrane Na^+-phosphate (P_i) cotransporter that is expressed in the proximal tubule where the bulk of filtered P_i is reabsorbed. Mice deficient in the *Npt2* gene were generated by targeted mutagenesis to define the role of *Npt2* in the overall maintenance of P_i homeostasis, determine its impact on skeletal development, and clarify its relationship to autosomal disorders of renal P_i reabsorption in humans. Homozygous mutants (*Npt2*$^{-/-}$) exhibit increased urinary P_i excretion, hypophosphatemia, an appropriate elevation in the serum concentration of 1,25-dihydroxyvitamin D with attendant hypercalcemia, hypercalciuria and decreased serum parathyroid hormone levels, and increased serum alkaline phosphatase activity. These biochemical features are typical of patients with hereditary hypophosphatemic rickets with hypercalciuria (HHRH), a Mendelian disorder of renal P_i reabsorption. However, unlike HHRH patients, *Npt2*$^{-/-}$ mice do not have rickets or osteomalacia. At weaning, *Npt2*$^{-/-}$ mice have poorly developed trabecular bone and retarded secondary ossification, but, with increasing age, there is a dramatic reversal and eventual overcompensation of the skeletal phenotype. Our findings demonstrate that *Npt2* is a major regulator of P_i homeostasis and necessary for normal skeletal development.**

Inorganic phosphate (P_i) is essential for a variety of cellular processes including skeletal mineralization. Because a disturbance in P_i availability can affect the functional integrity of many organ systems, specialized tissues have evolved to maintain the extracellular P_i concentration. In mammals, the regulation of P_i homeostasis is largely determined by the kidney, with 60–70% of the filtered P_i load reclaimed in the proximal segment of the nephron (1). Transepithelial transport of P_i from the renal lumen to the blood compartment involves uptake across the brush-border membrane (BBM), translocation across the cell, and efflux across the basolateral membrane (2). Evidence suggests that P_i transport across the BBM is the rate-limiting step in the overall P_i reabsorptive process and the major site for its regulation (2, 3). Kinetics studies demonstrated that the transport is mediated by high capacity, low affinity, and low capacity, high affinity Na^+–P_i cotransport systems (4).

Recently, cDNAs encoding two distinct low capacity, high affinity, renal BBM Na^+–P_i cotransporters (*NPT1* and *NPT2*) that share only 20% identity have been identified in several mammalian species by expression and homology cloning (5–13). *NPT2* is expressed exclusively in the proximal convoluted tubule and is regulated by P_i intake (14) and parathyroid hormone (PTH) (15), factors known to regulate renal BBM Na^+–P_i cotransport. In contrast, *NPT1* is expressed throughout the proximal tubule and is not subject to regulation by dietary P_i (10).

X-chromosome-linked and autosomal disorders of renal P_i reabsorption have been described in humans (16). Both are characterized by growth retardation, rachitic and osteomalacic bone disease, and hypophosphatemia, secondary to a renal defect in P_i reabsorption (17). Although renal *Npt2* gene expression is significantly reduced in the murine *Hyp* (18) and *Gy* (19) homologs of X-chromosome-linked hypophosphatemia, localization of the *NPT2*/*Npt2* gene to human chromosome 5q35 (20, 21) and mouse chromosome 13B (22) excluded it as a candidate gene. However, it is not yet clear whether mutations in *NPT2* are responsible for autosomal disorders of renal P_i wasting and mouse models for these disorders are not available.

To define the precise role of the NPT2 transporter in the overall maintenance of P_i homeostasis and to ascertain whether the phenotypic manifestations of autosomal hypophosphatemias can arise from mutations at the *NPT2* locus, we have disrupted the murine *Npt2* gene by homologous recombination in embryonic stem (ES) cells and introduced the mutation in the mouse germ line.

MATERIALS AND METHODS

Derivation of Mice Mutant for *Npt2*. A genomic clone encoding exons 2–12 of the *Npt2* gene, obtained by screening a λ DASH II mouse (129Sv strain) genomic DNA library with a rat *Npt2* cDNA probe (23), was used to generate a 2.2-kb *Eco*RI fragment encoding exons 2–5, and a 2.0-kb *Eco*RI–*Pst*I fragment containing part of intron 10 (Fig. 1*a*). The *Npt2* fragments were cloned into the pPNT plasmid (24), respectively, 5′ and 3′ of a neomycin resistance (*neo*^{r}) gene (Fig. 1*a*). The pPNT plasmid also contained a herpes simplex virus thymidine kinase (*hsv-tk*) gene, permitting selection against random integration. The resulting targeting vector, pPNT-Npt2 (Fig. 1*b*), was CsCl purified and linearized at the unique *Not*I site before electroporation.

Exponentially growing D3 ES cells (4.2×10^6) were electroporated (Bio-Rad Gene Pulser at 240 V, 500 μF) with 20 μg of pPNT-Npt2 as described (25) and selected in a medium containing 350 μg/ml G418 and 0.2 μM FIAU [1-(2-deoxy-2-fluoro-β-D-arabinofuranosyl)-5-iodouracil] for 5 days, and then for 3 more days with G418 alone. Genomic DNA was isolated from 170 doubly resistant ES cell clones, digested with *Eco*RI, transferred to supported nitrocellulose membranes [Optitran BA-(S)85, Schleicher & Schuell], and hybridized with probe A, located 3′ to the insertion point of the targeting

The publication costs of this article were defrayed in part by page charge payment. This article must therefore be hereby marked "*advertisement*" in accordance with 18 U.S.C. §1734 solely to indicate this fact.

This paper was submitted directly (Track II) to the *Proceedings* office.
Abbreviations: P_i, phosphate; BBM, brush-border membrane; PTH, parathyroid hormone; ES, embryonic stem cell; ALPase, alkaline phosphatase; $1,25(OH)_2D$, 1,25-dihydroxyvitamin D; FEI, fractional excretion index; HHRH, hereditary hypophosphatemic rickets with hypercalciuria; RT-PCR, reverse transcriptase–PCR.

§To whom reprint requests should be addressed at: Montreal Children's Hospital, 2300 Tupper Street, Montreal, PQ, Canada H3H 1P3. e-mail: mdht@musica.mcgill.ca.

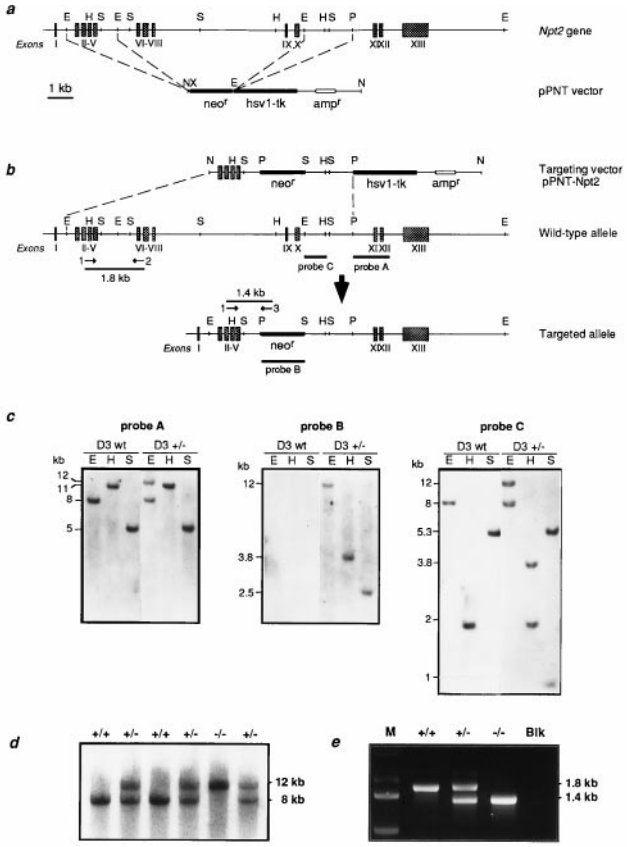

FIG. 1. Targeted disruption of the murine *Npt2* gene. (*a*) Production of the pPNT–Npt2 targeting vector. (*Upper*) Schematic representation of the murine *Npt2* gene, with exons numbered and denoted as grey boxes. (*Lower*) pPNT vector containing the *neo*^{r} and *hsv-tk* genes. The broken lines indicate sites where the *Npt2* homologous arms were inserted. Relevant restriction enzyme sites are abbreviated as follows: E, *Eco*RI; H, *Hin*dIII; N, *Not*I; P, *Pst*I; S, *Sst*I; X, *Xho*I. (*b*) Targeting of *Npt2* by homologous recombination. The top line represents the incoming pPNT–Npt2 targeting vector, the middle line the normal *Npt2* allele, and the bottom line the targeted allele. The location of the probes used in Southern blot analysis are indicated. Probe A, 1.5-kb fragment external to the targeting vector; probe B, corresponding to the *neo*^{r} gene; probe C, a 0.8-kb fragment used as an internal probe. (*c*) Southern blot analysis of targeted ES cell clones. Genomic DNA (5 μg) derived from untransfected ES cells (D3 wt) or from targeted clones (D3 +/−) was digested with *Eco*RI (E), *Hin*dIII (H), and *Sst*I (S), Southern blotted, and hybridized with probes A, B, and C, as shown. The sizes of genomic DNA fragments expected from the normal and disrupted alleles are indicated. (*d*) Genotyping of 3-week-old offspring from heterozygous matings by Southern blot analysis. Probe A was hybridized to *Eco*RI-restricted tail genomic DNA. Wild-type (+/+) and heterozygous (+/−) animals exhibited an 8-kb band that is absent in homozygous mutant (−/−) mice. Disruption of the *Npt2* allele produced a 12-kb band. (*e*) PCR analysis of mouse tail DNA from wild-type (+/+), heterozygous (+/−), and homozygous mutant (−/−) mice. Positions of the primers used for the PCR and the expected sizes of amplified fragments are indicated above the corresponding alleles in *b*. M, size markers; Blk, negative control.

vector (Fig. 1*b*) according to standard procedures (26). Seven positive clones were further analyzed by Southern blot analysis by using probes A, B, and C (Fig. 1*b*) after digestion of the DNA with three different restriction enzymes (Fig. 1*c*), and five clones with the predicted homologous integration were identified. Chimeric mice were generated from three different clones as described by Bradley (27). Briefly, 12–17 ES cells were injected into 3.5-day-old blastocysts obtained from naturally mated C57BL/6J females. The injected blastocysts were transferred to uteri of 2.5-day postcoitum, pseudopregnant CD1 recipients. Pups were born after 17 days and germ-line transmission of the mutation was determined by Southern blot analysis and PCR amplification of tail DNA (see below). To produce *Npt2*$^{-/-}$ mice, heterozygous offspring were intercrossed. The mice studied were of 129Sv and C57BL/6J mixed genetic background and maintained on Rodent Laboratory Chow (Ralston Purina, diet no. 5001) containing 1% calcium, 0.61% P_i, and 4.5 units of vitamin D_3/g. All experiments were conducted in accordance with the guidelines of the Canadian Council on Animal Care.

Genotyping of Mice. Mice were genotyped by Southern blot analysis and PCR. Genomic DNA was digested with *Eco*RI and analyzed by Southern blot hybridization using probe A (Fig. 1*b*). Expected sizes of fragments for the normal and disrupted alleles are 8 and 12 kb, respectively (Fig. 1*d*). PCR typing of tail DNA was performed by using *Taq* polymerase and 3 primers: sense primer 1 (5′-TGCCCAGGTTGGCACGAAGC-3′) in exon 4, antisense primer 2 (5′-AGTCCTGTCCCCTGCCTGCA-3′) in exon 6, and antisense primer 3 (5′-TGCTACTTCCATTTGTCACGTCC-3′) in the *neo*^{r} gene cassette (Fig. 1*b*). Expected sizes of amplified fragments are 1.8 kb for the normal allele (primers 1 and 2) and 1.4 kb for the disrupted allele (primers 1 and 3) (Fig. 1*e*).

Analysis of RNA. Total RNA (15 μg), isolated with TRIzol Reagent (GIBCO/BRL), was size fractionated on a 1.5% agarose/formaldehyde gel and transferred to Hybond-N nylon membranes (Amersham). The blots were probed as described (28) with a full-length rat *Npt2* cDNA and an 18S rRNA oligonucleotide. Filters were washed to high stringency, exposed to Kodak Biomax MR1 film at −80°C, and RNA abundance quantitated by densitometric analysis using an LKB Ultroscan Laser Densitometer under conditions where linearity was observed. For reverse transcriptase–PCR (RT-PCR), total RNA (5 μg) was reverse transcribed by using random hexamers and SuperScript reverse transcriptase (GIBCO/BRL), as recommended by the manufacturer. Primers 1 and 2 were used for detection of *Npt2* sequences.

BBM Vesicle Preparation, Western Blot Analysis, and Transport Studies. Renal BBM vesicles were prepared from kidney cortex by the $MgCl_2$ precipitation method as described (29) and used for both Western blot analysis and transport studies. BBM proteins were separated on 10% SDS/PAGE gels according to the method of Laemmli (30), transferred to supported nitrocellulose membranes (Hybond-C extra, Amersham), and probed sequentially with a rabbit polyclonal anti-rat Npt2 antibody (gift of H. Murer) (18) and a mAb raised against the α-subunit of rat meprin (gift of P. Crine) (31). Primary antibodies were visualized by using an enhanced chemiluminescence kit (Amersham). Quantitation of the signal was achieved by densitometric analysis using an LKB Ultroscan Laser Densitometer under conditions where linearity was observed.

The uptakes of P_i (100 μM) and glucose (10 μM), each performed in quadruplicate, were measured at 6 s, 30 s, 60 s, and 90 min in medium containing either 100 mM NaCl or 100 mM KCl by the rapid filtration technique described (29).

Serum and Urine Parameters. Serum P_i, Ca, and alkaline phosphatase (ALPase) activity and urine P_i, Ca, and creatinine were assayed on a Hitachi 917 automatic analyzer (Hitachi, Tokyo). The fractional excretion indexes FEI_{P_i} and FEI_{Ca} were calculated as follows: urine P_i or Ca/(urine creatinine × serum P_i or Ca). The serum concentration of 1,25-dihydroxyvitamin D [1,25$(OH)_2$D] was measured by using a calf thymus radioreceptor assay kit (Incstar, Stillwater, MN). The serum concentration of PTH was measured by using a rat PTH immunoradiometric assay kit (Nichols Institute, San Juan Capistrano, CA). Urine amino acids were determined on a Beckman 6300 amino acid analyzer (Beckman) and urine glucose and protein with Aimes Mulitistix (Miles).

Bone Histology. Tibiae from 21-, 45-, 74-, 115-, and 184-day-old mice were fixed in 4% paraformaldehyde in 0.1 M phosphate buffer (pH 7.4) at 4°C for 12 h and then decalcified in 10% EDTA

(pH 7.4) at 4°C for 10 days prior to dehydration with an increasing concentration of ethanol. Bones were then embedded in paraffin and sections were stained with haematoxylin/eosin. Number and length of trabeculae were determined in an area of 300 μm in length from the chondro-osseous junction to the diaphysis surrounded by cortical bone on both sides.

RESULTS

Targeted Disruption of the *Npt2* Gene. To inactivate the *Npt2* gene, we constructed a targeting vector in which *Npt2* genomic fragments, encoding exons 2–5 and intron 10, respectively, were cloned into the *Xho*I and *Eco*RI sites of the pPNT plasmid (24), 5′ and 3′ to the *neo*^{r} gene (Fig. 1*a*). A double cross-over event would lead to the replacement of 7.7 kb of the *Npt2* gene (corresponding to amino acids 178–389 of the Npt2 protein) with the *neo*^{r} gene (Fig. 1*b*). By using Southern blot analysis, 5 of 170 doubly resistant ES cell clones were found to have undergone homologous recombination, generating a 12-kb *Eco*RI fragment from the targeted allele and an 8-kb fragment from the normal allele (Fig. 1*c*).

Germ-line transmission of the inactivated *Npt2* allele resulted in mice heterozygous for the mutation. Southern blot analysis (Fig. 1*d*) and PCR (Fig. 1*e*) were used to genotype the offspring of heterozygous matings. From a total of 404 mice, 110 were wild type (27%), 200 were heterozygotes (50%), and 94 were homozygous mutants (23%), close to the expected Mendelian ratio (1:2:1), indicating the absence of prenatal homozygous lethality. However, of the 94 $Npt2^{-/-}$ mice genotyped, 41 (44%) died before or at weaning. This proportion was significantly higher than that observed for wild-type and heterozygous mice.

Phenotypic Features of *Npt2*-Deficient Mice. $Npt2^{-/-}$ mice were noticeably smaller than wild-type littermates and body weight was significantly reduced at birth (1.49 ± 0.08 g, $n = 8$ vs. 1.89 ± 0.12 g, $n = 11$, $P < 0.05$) and remained so for at least 4 months thereafter (Fig. 2). During the first 2 weeks of life, $Npt2^{-/-}$ mice showed apparent muscle weakness, some lethargy, and frequently had trouble feeding, suggesting that poor nutritional status likely contributed to their premature death. $Npt2^{-/-}$ mice that survived weaning appeared normal thereafter, despite smaller size and lower body weight (Fig. 2). $Npt2^{-/-}$ mice have a lower reproductive ability than wild-type and heterozygous animals.

Blood and urine parameters of $Npt2^{-/-}$ mice differed significantly from those of wild-type and heterozygous littermates (Table 1). The serum P_i concentration was markedly reduced at all ages examined and, in agreement with earlier work (32), decreased with age in all three genotypes (Table 1). The urine P_i/creatinine ratio and the fractional excretion index for P_i (FEI_{P_i}) were strikingly elevated in $Npt2^{-/-}$ mice (Table 1). In addition, homozygous mutants exhibited an appropriate elevation in serum $1,25(OH)_2D$ levels in response to hypophosphatemia (Table 1). At all ages examined, the serum concentration of calcium was slightly but significantly elevated in $Npt2^{-/-}$ mice and showed no age dependence (Table 1). The urine calcium/creatinine ratio and FEI_{Ca} were greatly increased and the serum PTH concentration was appropriately decreased in $Npt2^{-/-}$ mice (Table 1). There was no evidence for amino aciduria, glycosuria, or proteinuria in $Npt2^{-/-}$ mice (data not shown), indicating that a generalized tubulopathy was not responsible for the renal P_i leak in homozygous mutant mice.

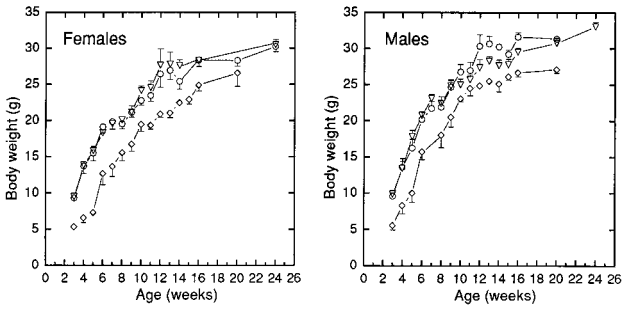

FIG. 2. Body weight of $Npt2^{+/+}$, $Npt2^{+/-}$, and $Npt2^{-/-}$ mice as a function of age. Normal mice and their mutant littermates were weighed between 3 weeks and 6 months of age. Each point represents mean ± SD derived from 4 to 30 measurements. $Npt2^{+/+}$ (○), $Npt2^{+/-}$ (▽), and $Npt2^{-/-}$ (◇) mice.

Serum ALPase activity decreased with age in young normal and mutant mice but, by 4 months of age, was no longer age dependent (Table 1). However, serum ALPase activity was significantly higher in young $Npt2^{-/-}$ mice than that in age-matched wild-type and heterozygous mice and, by 4 months of age, was comparable in all three genotypes (Table 1).

Heterozygous mice were indistinguishable from their wild-type littermates with respect to size, body weight (Fig. 2), behavior, and reproductive ability. However, a few differences in their blood and urine biochemical profiles were apparent (Table 1). Although $Npt2^{+/-}$ mice had a normal serum P_i concentration, their urine P_i/creatinine ratio and FEI_{P_i} were significantly elevated compared with wild-type mice (Table 1). $Npt2^{+/-}$ mice also exhibited elevated serum $1,25(OH)_2D$ levels (Table 1).

***Npt2* Gene Expression.** Northern blot analysis of total RNA isolated from bone, kidney, liver, and lung of animals from the three genotypes revealed the presence of a 2.6-kb transcript in the kidney of wild-type and heterozygous mice but not in the kidney of homozygous mutants (Fig. 3*a*). Quantitation of the 2.6-kb transcript, relative to 18S rRNA, indicated that $Npt2^{+/-}$ mice had ≈50% of the wild-type *Npt2* mRNA, consistent with the presence of only one functional *Npt2* allele. RT-PCR with *Npt2* primers also confirmed the absence of detectable renal *Npt2* mRNA in $Npt2^{-/-}$ mice (Fig. 3*b*). In agreement with previous work (8), *Npt2* transcripts were only detectable in the kidney (Fig. 3 *a* and *b*).

Western blot analysis of renal BBM proteins demonstrated the presence of an 86-kDa protein in $Npt2^{+/+}$ and $Npt2^{+/-}$ mice that was not detectable in homozygous mutants (Fig. 3*c*). Despite the reduction in *Npt2* mRNA expression in $Npt2^{+/-}$mice, the abundance of Npt2 protein, relative to that of meprin, was as prominent as in wild-type animals (Fig. 3*c*), consistent with the well-documented adaptive up-regulation of Npt2 protein in states of hypophosphatemia (14, 19, 33).

To assess the effect of the disrupted *Npt2* allele on functional activity, we examined the time course of Na^+–P_i cotransport in renal BBM vesicles isolated from $Npt2^{+/+}$, $Npt2^{+/-}$, and $Npt2^{-/-}$ mice. The Na^+-dependent component of P_i uptake at 6, 30, and 60 s is similar in BBM vesicles from wild-type and heterozygous mice but is reduced by 79%, 71%, and 69%, respectively, in mutant homozygotes (Fig. 3*d*). However, at equilibrium (90 min), when the Na^+-gradient has dissipated, P_i uptake is comparable in all three groups of mice (Fig. 3*d*). Moreover, the Na^+-independent component of P_i uptake (Fig. 3*d*) and Na^+-dependent and independent glucose uptake, measured in parallel (data not shown), were also similar in all three genotypes.

Skeletal Phenotype of *Npt2*-Deficient Mice. Histological analysis of tibial sections from 21-day-old animals revealed that $Npt2^{-/-}$ mice have poorly developed metaphyseal trabeculae and retarded secondary ossification in the epiphysis when compared with wild-type littermates (Fig. 4*a*). In $Npt2^{+/-}$ mice, these features are intermediate between wild-type and homozygous littermates (Fig. 4*a*). At 21 days of age, both the length (+/+, 163 ± 31; +/−, 127 ± 33; −/−, 98 ± 15; mean ± SD, μm; +/− vs. +/+, $P < 0.01$; −/− vs. +/+, $P < 0.005$) and number (+/+, 41 ± 3; +/−, 37 ± 5; −/−, 21 ± 3; mean ± SD; +/− vs. +/+, not significant; −/− vs. +/+, $P < 0.005$) of metaphyseal trabeculae are decreased in homozygous mutants and intermediate in heterozygotes when compared with wild-type littermates. In addition, differences in osteoclast (tartrate-resistant acid phosphatase positive cells) distribution and osteopontin-immunopositive bone surfaces as well as a

Table 1. Blood and urine profiles for $Npt2^{+/+}$, $Npt2^{+/-}$, and $Npt2^{-/-}$ mice

	Age, months	$Npt2^{+/+}$ (n)	$Npt2^{+/-}$ (n)	$Npt2^{-/-}$ (n)
Serum P_i, mM	1	2.87 ± 0.07 (20)	2.78 ± 0.06 (37)	1.86 ± 0.08 (11)**
	2	2.35 ± 0.09 (6)	2.41 ± 0.06 (6)	1.79 ± 0.06 (7)**
	3	2.10 ± 0.08 (9)	2.30 ± 0.08 (9)	1.77 ± 0.10 (7)*
	4	2.10 ± 0.07 (6)	2.08 ± 0.18 (6)	1.65 ± 0.14 (4)*
	5	1.94 ± 0.14 (6)	1.97 ± 0.10 (7)	1.58 ± 0.03 (4)*
	6	1.85 ± 0.09 (5)	2.02 ± 0.08 (7)	ND
	7	1.79 ± 0.08 (4)	1.88 ± 0.13 (5)	ND
Urine P_i/creatinine†		9.83 ± 1.15 (26)	16.62 ± 1.61 (37)*	24.98 ± 2.02 (21)**
FEI_{P_i}‡		4.22 ± 0.63 (16)	6.79 ± 0.75 (28)*	13.24 ± 1.08 (9)**
Serum total Ca^{2+}, mM	1	2.25 ± 0.03 (20)	2.21 ± 0.03 (34)	2.64 ± 0.05 (12)**
	2	2.19 ± 0.04 (5)	2.21 ± 0.03 (6)	2.36 ± 0.05 (7)*
	3	2.20 ± 0.05 (9)	2.13 ± 0.06 (8)	2.41 ± 0.08 (10)*
	4	2.26 ± 0.03 (6)	2.24 ± 0.05 (6)	2.42 ± 0.04 (3)*
	5	2.00 ± 0.12 (5)	2.13 ± 0.05 (7)	2.48 ± 0.02 (3)*
	6	2.22 ± 0.09 (3)	2.32 ± 0.09 (8)	ND
	7	2.40 ± 0.06 (2)	2.23 ± 0.04 (3)	ND
Urine Ca^{2+}/creatinine†		0.81 ± 0.07 (23)	1.00 ± 0.12 (36)	7.90 ± 1.07 (20)**
FEI_{Ca^+}‡		0.36 ± 0.04 (15)	0.52 ± 0.07 (27)	3.43 ± 0.46 (10)**
Serum $1,25(OH)_2D$,§ pg/ml		36.3 ± 9.5 (3)	73.0 ± 7.2 (3)*	107.3 ± 11.1 (3)**
Serum PTH,¶ pg/ml		18.83 ± 1.14 (3)	19.79 ± 2.31 (3)	6.98 ± 0.60 (3)**
Serum ALPase, units/liter	1	425 ± 35 (19)	459 ± 22 (32)	869 ± 165 (12)**
	2	179 ± 28 (4)	208 ± 19 (6)	361 ± 17 (7)**
	3	126 ± 9 (9)	99 ± 7 (9)	175 ± 15 (8)*
	4	91 ± 6 (6)	82 ± 8 (6)	105 ± 10 (4)
	5	71 ± 14 (5)	63 ± 3 (7)	98 ± 7 (3)
	6	92 ± 5 (3)	64 ± 10 (7)	ND
	7	84 ± 0 (2)	61 ± 12 (3)	ND

Results are means ± SEM (n, number of mice analyzed). ND, test not performed. *, $P = 0.05$–0.01 for t test comparing mutant mice to $Npt2^{+/+}$ mice. **, $P < 0.01$ for t test comparing mutant mice to $Npt2^{+/+}$ mice.
†Assays were done on urine collected from 1- to 3-month-old animals.
‡FEI indicates the ratio between urine P_i or Ca (mM)/{urine creatinine (mM) × serum P_i or Ca (mM)} (1-month-old animals).
§$1,25(OH)_2D$ assays were done in duplicate on three serum pools from six mice each (1- to 3-month-old animals).
¶PTH assays were done in duplicate on three serum pools from two or three mice each (2- to 3-month-old animals).

decrease in osteoclast number are apparent in tibiae of 21-day-old $Npt2^{-/-}$ mice and wild-type littermates, suggestive of a defect in bone remodeling in the homozygous mutants (data not shown).

In contrast, tibial sections from 45-day-old mice failed to demonstrate the genotype differences evident at 21 days of age (data not shown). At 115 days of age, however, the number of metaphyseal trabeculae in $Npt2^{-/-}$ mice is significantly greater than that of $Npt2^{+/+}$ littermates (+/+, 16 ± 3; +/−, 21 ± 3; −/−, 25 ± 3; mean ± SD; +/− vs. +/+, $P < 0.05$; −/− vs. +/+, $P < 0.005$) and the area of epiphyseal bone marrow in the homozygous mutants is partially occupied with calcified bone (Fig. 4*b*). Similar findings are observed at 74 and 184 days of age (data not shown).

DISCUSSION

We demonstrate that *Npt2*-deficient mice exhibit increased urinary P_i excretion, hypophosphatemia, and an appropriate adaptive increase in the circulating concentration of $1,25-(OH)_2D$. Additional biochemical findings in $Npt2^{-/-}$ mice include hypercalcemia, hypercalciuria, decreased serum PTH levels, and elevated serum ALPase activity. These biochemical features are typical of patients with hereditary hypophosphatemic rickets with hypercalciuria (HHRH), a Mendelian disorder of renal P_i reabsorption (17). In contrast to patients with HHRH, $Npt2^{-/-}$ mice do not exhibit rickets and osteomalacia. Rather, the mutant homozygotes have a complex bone phenotype with retarded secondary ossification at weaning followed by a reversal and eventual overcompensation of the early bone phenotype with increasing age.

The phenotypic features that characterize $Npt2^{-/-}$ mouse are likely the direct consequence of impaired renal P_i reabsorption, secondary to the loss of *Npt2* function in the kidney. This conclusion is based on the report that *Npt2* is expressed exclusively in the kidney (8) and is confirmed by the present findings. We were unable to detect *Npt2* mRNA expression in bone, liver, and lung of normal mice by either Northern blot analysis or RT-PCR. In addition, by using a RNase protection assay, we did not detect *Npt2* transcripts in mouse intestine (data not shown), a tissue that has considerable morphological and functional similarity to the renal epithelium. Accordingly, the molecular entities that mediate Na^+–P_i cotransport in tissues other than the kidney are distinct from *Npt2* and, as such, would not contribute to the mutant phenotype.

We demonstrate that BBMs from $Npt2^{-/-}$ mice retain 20–30% of the Na^+-P_i cotransport activity expressed in wild-type mice. Our data indicate that gene products other than *Npt2* mediate Na^+–P_i cotransport at the apical surface of the murine proximal nephron. Likely candidates for this activity are *Npt1* (7) *Ram-1* and *Glvr-1* (34). Indeed, *Npt1* expression was previously localized to the renal BBM of proximal tubular cells (35, 36). In addition, it has been shown that *Ram*-1 and *Glvr*-1, ubiquitous cell surface viral receptors that mediate high affinity, Na^+-dependent P_i transport, are expressed in kidney (34). At present, little is known about the relative contribution of *Npt1*, *Ram-1*, and *Glvr-1* to overall renal BBM Na^+–P_i cotransport. However, our data in homozygous mutant mice suggest that Npt2 accounts for ≈70% of BBM P_i transport activity. Although these results are consistent with the relative distribution of *Npt1, Npt2, Ram-1*, and *Glvr-1* mRNAs in normal mouse kidney (37), it is not clear whether *Npt*1-, *Ram*-1- or *Glvr*-1-mediated Na^+-P_i cotransport is up-regulated in the absence of Npt2 activity.

P_i is an important determinant of $1,25(OH)_2D$ synthesis in the kidney. P_i deprivation elicits an adaptive increase in the activity of the renal biosynthetic enzyme, 25-hydroxyvitamin D-1-

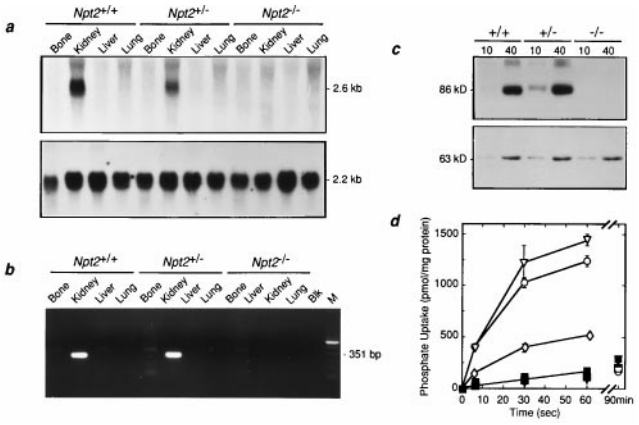

FIG. 3. *Npt2* gene expression. (*a*) Northern blot analysis of total RNA from bone, kidney, liver, and lung of $Npt2^{+/+}$, $Npt2^{+/-}$ and $Npt2^{-/-}$ mice. Total RNA (15 μg) was blotted to a nylon membrane and hybridized sequentially with ^{32}P-labeled rat *Npt2* cDNA (*Upper*) and 18S rRNA oligonucleotide (*Lower*) probes as described. (*b*) RT-PCR of total RNA from $Npt2^{+/+}$, $Npt2^{+/-}$, and $Npt2^{-/-}$ mice. Total RNA (5 μg) from bone, kidney, liver, and lung was reverse transcribed and PCR amplified as described. An aliquot of each PCR was electrophoresed on 1.5% agarose gels and visualized with ethidium bromide. M, size markers, Blk, negative control. (*c*) Western blot analysis of renal BBM proteins from $Npt2^{+/+}$, $Npt2^{+/-}$, and $Npt2^{-/-}$ mice. The BBMs were solubilized and subjected to SDS/PAGE, transferred to nitrocellulose, and the blots probed sequentially with (*Upper*) a rabbit polyclonal anti-rat Npt2 antibody and (*Lower*) a mAb raised against the α-subunit of rat meprin. Molecular masses and quantity of protein (μg) applied to each lane are indicated. (*d*) P_i uptake in renal BBM vesicles from $Npt2^{+/+}$, $Npt2^{+/-}$, and $Npt2^{-/-}$ mice. P_i uptake (100 μM) was measured at times indicated in presence of KCl (filled symbols) and NaCl (open symbols) in BBM vesicles derived from $Npt2^{+/+}$ (circles), $Npt2^{+/-}$ (triangles), and $Npt2^{-/-}$ (diamond) mice as described. Each point represents mean ± SEM of quadruplicate determinations.

hydroxylase (38, 39), which in turn leads to a corresponding increase in serum $1,25(OH)_2D$ levels (40). In the present study, we demonstrate that hypophosphatemia, secondary to abrogation

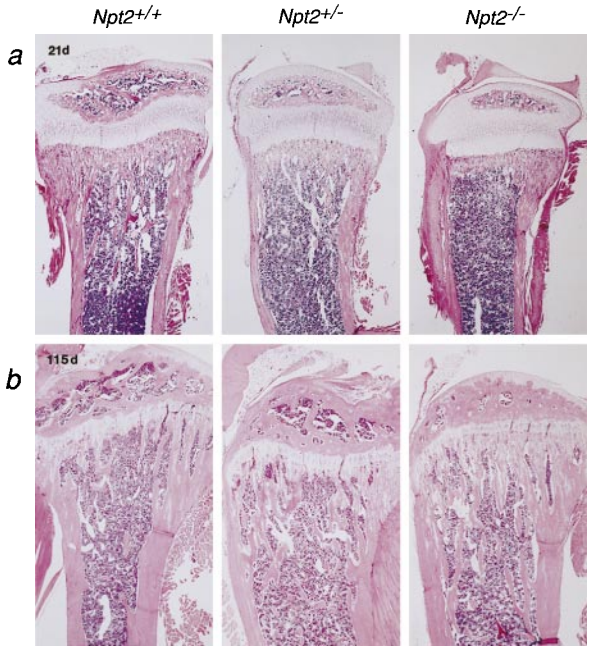

FIG. 4. Histological appearance of bone from $Npt2^{+/+}$, $Npt2^{+/-}$, and $Npt2^{-/-}$ mice. Longitudinal tibial sections were prepared from 21- (*a*) and 115-day-old (*b*) mice as described and stained with hematoxylin/eosin.

of renal *Npt2* function, is also associated with a significant rise in the serum concentration of $1,25(OH)_2D$, thereby confirming the regulatory loop between extracellular P_i and renal vitamin D hormone synthesis. Previous studies have shown that the increase in $1,25(OH)_2D$ elicits a marked stimulation in intestinal P_i (41) and calcium (42) absorption. Intestinal P_i hyperabsorption in *Npt2* null mice would result in an increase in the filtered P_i load that, together with *Npt2* ablation, is responsible for the substantial elevation in urinary P_i excretion. Intestinal calcium hyperabsorption in *Npt2* null mice would lead to hypercalcemia, an increase in the filtered calcium load, and a suppression of PTH secretion, which contribute to the significant hypercalciuria observed in the homozygous mutant mice.

The phenotype of $Npt2^{+/-}$ mice is of considerable interest. $Npt2^{+/-}$ mice grow normally and are able to maintain normal serum P_i levels in the face of a modest increase in urinary P_i excretion. Moreover, the heterozygotes exhibit normal BBM Na^+–P_i cotransport activity and an abundance of Npt2 protein that is comparable to that in wild-type mice in spite of a 50% reduction in *Npt2* mRNA. These findings are likely the result of an adaptive response to the loss of one copy of the *Npt2* gene. Previous studies have shown that renal BBM Na^+–P_i cotransport and Npt2 cotransporter protein are both upregulated by hypophosphatemia following low P_i challenge (14, 33). Although the renal P_i sensing mechanism that is involved in initiating the adaptive response to P_i deprivation has not yet been defined, our data suggest that kidneys of $Npt2^{+/-}$ mice are able to react appropriately to the increase in renal P_i loss and the resulting perturbation in P_i homeostasis.

Mice homozygous for the disrupted *Npt2* gene have the biochemical features of patients with HHRH (43–47), yet the bone phenotype is markedly different in the human and mouse disorders. Children with HHRH present with radiological features of rickets, and adult patients with histomorphometric findings that are consistent with osteomalacia, such as irregular mineralization fronts, markedly elevated osteoid surface and seam width, increased number of osteoid lamellae, and prolonged mineralization time (48). In contrast, it does not appear from preliminary observations that the skeletal phenotype in $Npt2^{-/-}$ mice is similar to that in HHRH patients. There are several explanations for this discrepancy. (*i*) The bone response to hypophosphatemia and the P_i requirement for skeletal mineralization may differ substantially in humans and mice. Indeed, basal serum P_i levels are markedly different in the two species. (*ii*) Bone responses to elevated $1,25(OH)_2D$ levels may differ in both species. The latter is suggested by a recent report showing differences in the regulation of human and murine osteocalcin gene expression by $1,25(OH)_2D$ (49). (*iii*) A mutation in the *NPT2* gene may not be the cause of HHRH.

The bone findings in mice homozygous for the disrupted *Npt2* allele are clearly age dependent. With increasing age, $Npt2^{-/-}$ mice exhibit a dramatic reversal and eventual overcompensation of the skeletal changes apparent at 21 days of age. These differences may be attributed to age-related differences in the bone and intestinal response to $1,25(OH)_2D$. Recent studies in vitamin D receptor (VDR) null mice suggest that the phenotypic consequences of VDR ablation are not evident until after weaning, suggesting that $1,25(OH)_2D$ may not play an important physiological role before 21 days of age (50, 51). Accordingly, osteoblast and osteoclast activity and intestinal P_i absorption may not be responsive to the elevated circulating levels of $1,25(OH)_2D$ in $Npt2^{-/-}$ mice before weaning, whereas after weaning, $1,25(OH)_2D$/VDR-dependent compensatory changes in intestinal P_i absorption and bone mineralization can occur. Further studies are necessary to determine whether this or other mechanisms contribute to the age-related differences in the bone phenotype of $Npt2^{-/-}$ mice.

We demonstrate that $Npt2^{-/-}$ mice have decreased circulating levels of PTH relative to wild-type littermates. Because PTH increases both osteoclast number and activity, reduced

serum PTH levels in *Npt2* null mice may contribute to compromised osteoclast function and a consequent bone remodeling defect. Preliminary data suggest that osteoclast number as well as tartrate-resistant acid phosphatase-positive and osteopontin-immunopositive cement lines are decreased in tibiae of 21-day $Npt2^{-/-}$ mice, relative to wild-type littermates, consistent with the notion that bone remodeling is impaired in young homozygous mutants.

In summary, we have demonstrated that mice homozygous for the disrupted *Npt2* gene exhibit many of the features of HHRH and that the *Npt2* gene plays an essential role in the regulation of P_i homeostasis and in normal skeletal development and growth. We believe that $Npt2^{-/-}$ mice provide a unique animal model to define the effects of disturbed P_i homeostasis not only on the skeleton but also on a variety of organ systems where P_i plays a crucial role and in disease states where aberrant P_i economy is manifest.

We thank Drs. H. Murer and J. Biber (University of Zurich) for the gift of the Npt2 antibody, Dr. P. Crine (University of Montreal) for the gift of the meprin mAb, and Hannah Hoag for critical review of the manuscript. This work was supported by grants from the Medical Research Council of Canada (Medical Research Council Group Grant in Medical Genetics to H.S.T. and Medical Research Council Grant to A.C.K.). L.B. was the recipient of Fellowship Awards from the McGill University-Montreal Children's Hospital Research Institute and the Medical Research Council of Canada.

1. Mizgala, C. L. & Quamme, G. A. (1985) *Physiol. Rev.* **65,** 431–466.
2. Murer, H., Werner, A., Reshkin, S., Wuarin, R. & Biber, J. (1991) *Am. J. Physiol.* **260,** C885–C899.
3. Berndt, T. J. & Knox, F. G. (1992) in *The Kidney: Physiology and Pathophysiology*, eds. Seldin, D. W. & Giebisch, G. (Raven, New York), pp. 2511–2532.
4. Walker, J. J., Yan, T. S. & Quamme, G. A. (1987) *Am. J. Physiol.* **252,** F226–F231.
5. Werner, A., Moore, M. L., Mantei, N., Biber, J., Semenza, G. & Murer, H. (1991) *Proc. Natl. Acad. Sci. USA* **88,** 9608–9612.
6. Chong, S. S., Kristjansson, K., Zoghbi, H. Y. & Hughes, M. R. (1993) *Genomics* **18,** 355–359.
7. Chong, S. S., Kozak, C. A., Liu, L., Kristjansson, K., Dunn, S. T., Bourdeau, J. E. & Hughes, M. R. (1995) *Am. J. Physiol.* **268,** F1038–F1045.
8. Magagnin, S., Werner, A., Markovich, D., Sorribas, V., Stange, G., Biber, J. & Murer, H. (1993) *Proc. Natl. Acad. Sci. USA* **90,** 5979–5983.
9. Sorribas, V., Markovich, D., Hayes, G., Stange, G., Forgo, J., Biber, J. & Murer, H. (1994) *J. Biol. Chem.* **269,** 6615–6621.
10. Verri, T., Markovich, D., Perego, C., Norbis, F., Stange, G., Sorribas, V., Biber, J. & Murer, H. (1995) *Am. J. Physiol.* **268,** F626–F633.
11. Collins, J. F. & Ghishan, F. K. (1994) *FASEB J.* **8,** 862–868.
12. Hartmann, C. M., Wagner, C. A., Busch, A. E., Markovich, D., Biber, J., Lang, F. & Murer, H. (1995) *Pflügers Arch.* **430,** 830–836.
13. Helps, C., Murer, H. & McGivan, J. (1995) *Eur. J. Biochem.* **228,** 927–930.
14. Levi, M., Lotscher, M., Sorribas, V., Custer, M., Arar, M., Kaissling, B., Murer, H. & Biber, J. (1994) *Am. J. Physiol.* **267,** F900–F908.
15. Kempson, S. A., Lotscher, M., Kaissling, B., Biber, J., Murer, H. & Levi, M. (1995) *Am. J. Physiol.* **268,** F784–F791.
16. McKusick, V. A. (1992) *Mendelian Inheritance in Man* (Johns Hopkins Univ. Press, Baltimore).
17. Rasmussen, H. & Tenenhouse, H. S. (1995) in *The Molecular and Metabolic Basis of Inherited Diseases*, eds. Scriver, C. R., Beaudet, A. L., Sly, W. S. & Valle, D. (McGraw-Hill, New York), pp. 3717–3745.
18. Tenenhouse, H. S., Werner, A., Biber, J., Ma, S., Martel, J., Roy, S. & Murer, H. (1994) *J. Clin. Invest.* **93,** 671–676.
19. Beck, L., Meyer, R. A., Jr., Meyer, M. H., Biber, J., Murer, H. & Tenenhouse, H. S. (1996) *Pflügers Arch.* **431,** 936–941.
20. Kos, C. H., Tihy, F., Econs, M. J., Murer, H., Lemieux, N. & Tenenhouse, H. S. (1994) *Genomics* **19,** 176–177.
21. McPherson, J. D., Krane, M. C., Wagner-McPherson, C. B., Kos, C. H. & Tenenhouse, H. S. (1997) *Pediatr. Res.* **41,** 632–634.
22. Zhang, X. X., Tenenhouse, H. S., Hewson, A. S., Murer, H. & Eydoux, P. (1997) *Cytogenet. Cell Genet.* **77,** 304–305.
23. Hartmann, C. M., Hewson, A. S., Kos, C. H., Hilfiker, H., Soumoumou, Y., Murer, H. & Tenenhouse, H. S. (1996) *Proc. Natl. Acad. Sci. USA* **93,** 7409–7414.
24. Tybulewicz, V. L. J., Crawford, C. E., Jackson, P. K., Bronson, R. T. & Mulligan, R. C. (1991) *Cell* **65,** 1153–1163.
25. Karaplis, A. C., Luz, A., Glowacki, J., Bronson, R. T., Tybulewicz, V. L. J., Kronenberg, H. M. & Mulligan, R. C. (1994) *Genes Dev.* **8,** 277–289.
26. Sambrook, J., Fritsch, E. F. & Maniatis, T. (1989) *Molecular Cloning: A Laboratory Manual* (Cold Spring Harbor Lab. Press, Plainview, NY), 2nd Ed.
27. Bradley, A. (1987) in *Teratocarcinomas and Embryonic Stem Cells: A Practical Approach*, ed. Robertson, E. J. (IRL, Washington, DC), pp. 113–152.
28. Beck, L., Soumounou, Y., Martel, J., Krishnamurthy, G., Gauthier, C., Goodyer, C. & Tenenhouse, H. S. (1997) *J. Clin. Invest.* **99,** 1200–1209.
29. Tenenhouse, H. S. & Scriver, C. R. (1978) *Can. J. Biochem.* **56,** 640–646.
30. Laemmli, U. K. (1970) *Nature (London)* **227,** 680–685.
31. Corbeil, D., Milhiet, P., Simon, V., Ingram, J., Kenny, A. J., Boileau, G. & Crine, P. (1993) *FEBS Lett.* **335,** 361–366.
32. Eicher, E. M., Southard, J. L., Scriver, C. R. & Glorieux, F. H. (1976) *Proc. Natl. Acad. Sci. USA* **73,** 4667–4671.
33. Tenenhouse, H. S., Martel, J., Biber, J. & Murer, H. (1995) *Am. J. Physiol.* **268,** F1062–F1069.
34. Kavanaugh, M. P., Miller, D. G., Zhang, W., Law, W., Kozak, S. L., Kabat, D. & Miller, A. D. (1994) *Proc. Natl. Acad. Sci. USA* **91,** 7071–7075.
35. Biber, J., Custer, M., Werner, A., Kaissling, B. & Murer, H. (1993) *Pflügers Arch.* **424,** 210–215.
36. Custer, M., Meier, F., Schlatter, E., Greger, R., Garcia-Perez, A., Biber, J. & Murer, H. (1993) *Pflügers Arch.* **424,** 203–209.
37. Tenenhouse, H. S., Roy, S. & Martel, J. (1997) *J. Am. Soc. Nephrol.* **8,** 568A (abstr.).
38. Baxter, L. A. & DeLuca, H. F. (1976) *J. Biol. Chem.* **251,** 3158–3161.
39. Gray, R. W. & Napoli, J. L. (1983) *J. Biol. Chem.* **258,** 1152–1155.
40. Tenenhouse, H. S. & Jones, G. (1990) *J. Clin. Invest.* **85,** 1450–1455.
41. Cross, H. S., Debiec, H. & Peterlik, M. (1990) *Miner. Electrolyte Metab.* **16,** 115–124.
42. van Os, C. H. (1987) *Biochim. Biophys. Acta* **906,** 195–222.
43. Tieder, M., Modai, D., Samuel, R., Arie, R., Halabe, A., Bab, I., Gabizon, D. & Lieberman, U. A. (1985) *N. Engl. J. Med.* **312,** 611–617.
44. Tieder, M., Modai, D., Shaked, U., Samuel, R., Arie, R., *et al.* (1987) *N. Engl. J. Med.* **316,** 125–129.
45. Proesmans, W. C., Fabrey, G., Marchal, G. J., Gillis, P. L. & Bouillon, R. (1987) *Pediatr. Nephrol.* **1,** 479–484.
46. Chen, C., Carpenter, T., Steg, N., Baron, R. & Anast, C. (1989) *Pediatrics* **84,** 276–280.
47. Tieder, M., Arie, R., Bab, I., Maor, J. & Liberman, U. A. (1992) *Nephron* **62,** 176–181.
48. Gazit, D., Tieder, M., Liberman, U. A., Passi-Even, L. & Bab, I. A. (1991) *J. Clin. Endocrinol. Metab.* **72,** 229–235.
49. Clemens, T. L., Tang, H., Maeda, S., Kesterson, R. A., Demayo, F., Pike, J. W. & Gundberg, C. M. (1997) *J. Bone Miner. Res.* **12,** 1570–1576.
50. Yoshizawa, T., Handa, Y., Uematsu, Y., Takeda, S., Sekine, K., *et al.* (1997) *Nat. Genet.* **16,** 391–396.
51. Li, Y. C., Pirro, A. E., Amling, M., Delling, G., Baron, R., Bronson, R. & Demay, M. B. (1997) *Proc. Natl. Acad. Sci. USA* **94,** 9831–9835.